

Supporting Information

Interaction of Water with the Gypsum (010) Surface: Structure and Dynamics from Nonlinear Vibrational Spectroscopy and Ab Initio Molecular Dynamics

Jaciara C. C. Santos,^{a,§} Fabio R. Negreiros,^{b,§,#} Luana S. Pedroza,^b Gustavo M. Dalpian,^b
Paulo B. Miranda^{a,*}

^a Instituto de Física de São Carlos, Universidade de São Paulo, CP 369, São Carlos-SP, 13560-970, Brazil

^b Centro de Ciências Naturais e Humanas, Universidade Federal do ABC, Santo André-SP, 09210-580,
SP, Brazil

[#] Current address: Departamento de Química Teórica y Computacional, Facultad de Ciencias Químicas,
Universidad Nacional de Córdoba, 5000, Cordoba, Argentina.

* Corresponding author. E-mail: miranda@ifsc.usp.br, tel: +55-16-33739825.

§ These authors contributed equally to this work.

1) Surface energy with and without structural water.

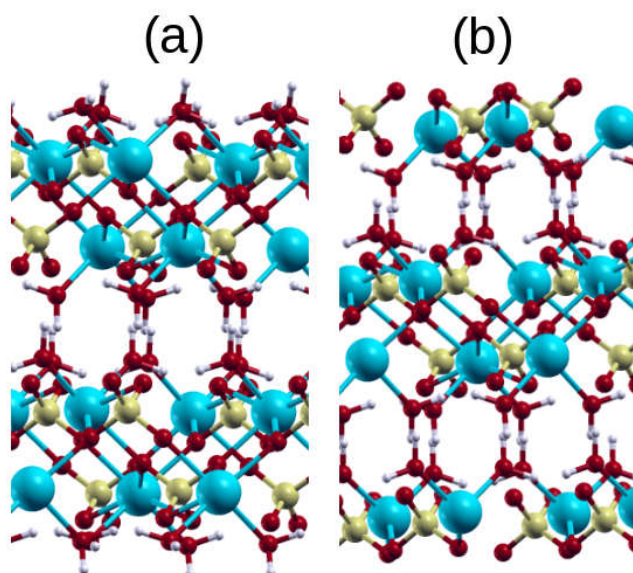


Fig. S1 – Relaxed gypsum slab with a surface in the (010) direction with two possible terminations, (a) with, and (b) without a single water monolayer. The evaluated surface energy for structures (a) and (b) is $14 \text{ meV}/\text{\AA}^2$ and $41 \text{ meV}/\text{\AA}^2$, respectively.

2) Snapshots of non-relaxed and optimized surfaces at different coverages.

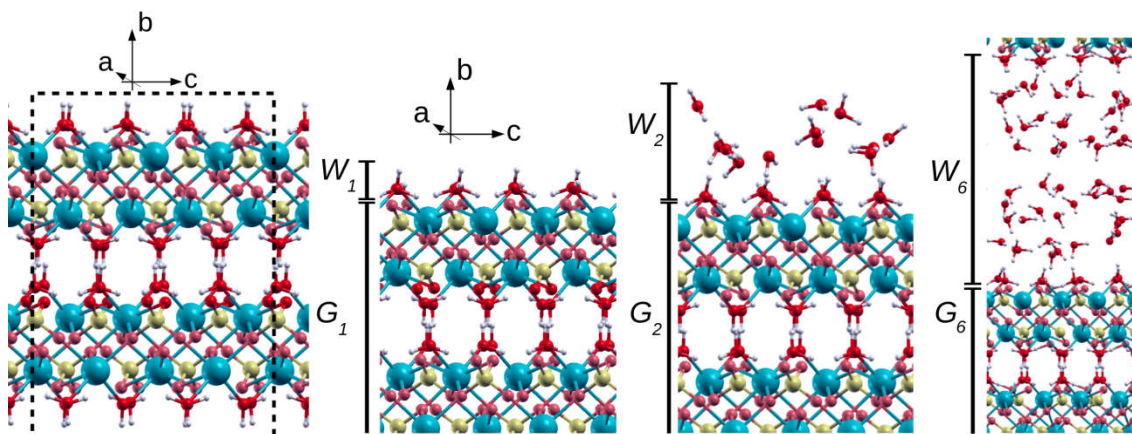


Fig. S2 – On the left, a view of the complete supercell for the unrelaxed 1ML case. On the right, the three figures show the optimized (010) surface with 1 ML, 2 ML, 6 ML coverages.

3) Power spectrum of confined water for all simulated structures

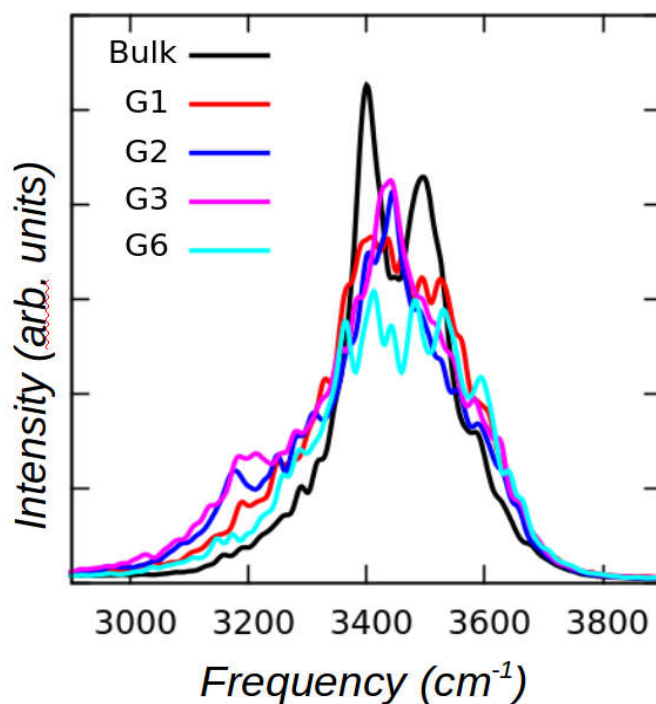


Fig. S3 – Confined “bulk” water contribution to the power spectrum for the gypsum structures: bulk (i.e., without a surface), and for the gypsum structure with different surface water coverages (G1, G2, G3 and G6 in Fig. S2). The surface water coverage does not significantly change this contribution, although noticeable differences can be seen. The calculated spectra in the main text refer only to surface water molecules (regions W_1 , W_2 and W_6 in Fig. S2).

4) Surface contribution dominates the SFG spectrum in reflection.

The SFG measurements were initially made with a thin sample (~ 1 mm), for which it is not possible to separate the reflections from the two gypsum/air interfaces. In this case, the detected signal is not only coming from that generated on the first air/gypsum interface in reflection, but also from that generated on the first interface in transmission, which is then partially reflected by the second gypsum/air interface (see Fig. S4d). If there is a contribution of the bulk crystal to the SFG signal, it will be significantly amplified in transmission due to the longer coherence length.¹ Thus, the signal generated in the bulk may be dominant if the sample is thin enough such that both reflections are detected. We have also performed measurements with a thicker sample (~ 7 mm) for which only the first reflection is measured (see Fig S4d), and a comparison of the two measurements is shown in Fig. S4a. It is clear that the only difference resulting from appreciable bulk contribution in transmission (for the thin sample) is a narrow peak at ~ 3450 cm^{-1} , which completely disappears for the thick sample, where only the SFG signal in the reflection geometry is collected. Note that the frequency of this bulk contribution coincides with that obtained by the MD simulations for the bulk structural water (Fig. S3), except that the experimental peak is narrower, perhaps due to gain narrowing.

Further confirmation that the SFG signal (apart from the narrow peak at ~ 3450 cm^{-1} in transmission) is coming from the gypsum/vapor interface comes from SFG measurements using deuterated water vapor. H-D exchange of surface water is observed when we add D_2O vapor to the chamber (Fig. S4b), as the OH stretch modes of adsorbed water ($3000 - 3400$ cm^{-1}) shift to lower OD stretch frequencies ($2300 - 2700$ cm^{-1}). As expected, this exchange is observed only for the interfacial water, since the intense peak attributed to bulk structural water (3450 cm^{-1}) is not affected. However, Fig. S4c shows that after this H-D exchange by exposure to D_2O vapor, if the chamber is opened and the crystal is exposed to air (H_2O vapor), the surface structural water is again exchanged back to H_2O . Therefore, as expected due to fast H-D exchange, it is not possible to use D_2O vapor to distinguish adsorbed water from the surface structural water present on the dry, cleaved gypsum surface, as done previously for water adsorption on mica.² Fig. S5 displays similar measurements, but with a thick sample that presents only the surface water contribution (both structural and adsorbed water). In this case, the spectrum from surface structural water at low RH (black circles, similar to Fig. 3 of the main text) presents a narrow peak at 3670 cm^{-1} due to free OH groups and a broad band at ~ 3250 cm^{-1} due to H-bonded OH groups. Upon D_2O adsorption (blue squares), we observe only OD stretches due to H-bonded OD groups at ~ 2500 cm^{-1} , without any free OD contribution. This spectrum resembles those with H_2O adsorption at high RH (Fig. 6), but red shifted to the OD stretch range. If we flow N_2 through the chamber to remove adsorbed D_2O , the surface is left only with structural D_2O water and the spectrum (red triangles) resembles that before D_2O adsorption at low RH (black circles), but red shifted to the OD stretch range. Finally, if this surface is exposed to air containing H_2O vapor (pink empty circles), the spectrum shifts back to the OH stretch range keeping the same spectral shape of the structural water contribution, containing both H-bonded and free OH groups.

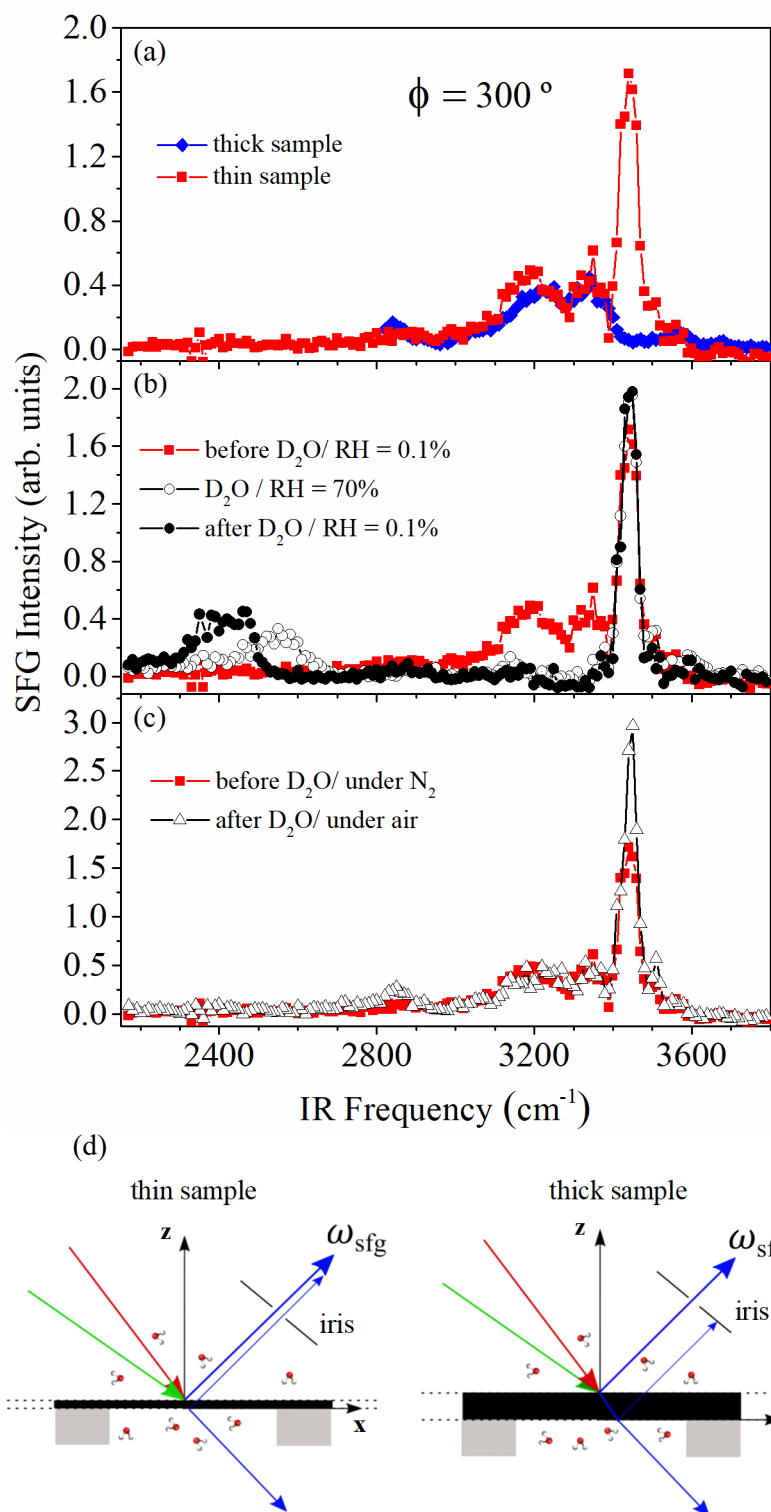


Fig. S4 – SFG spectra for the gypsum (010)/vapor interface in the OD and OH stretch ranges for the azimuthal angle $\phi = 300^\circ$ and SSP polarization combination. (a) Thin vs. thick sample under low humidity (RH = 0.1%). (b) Thin sample before, during (RH = 70%) and after D_2O adsorption. (c) Thin sample before and after D_2O adsorption, but with the crystal exposed to atmospheric air (containing H_2O vapor). (d) Scheme of the experimental geometry for detecting the SFG signals from a thin or thick gypsum sample.

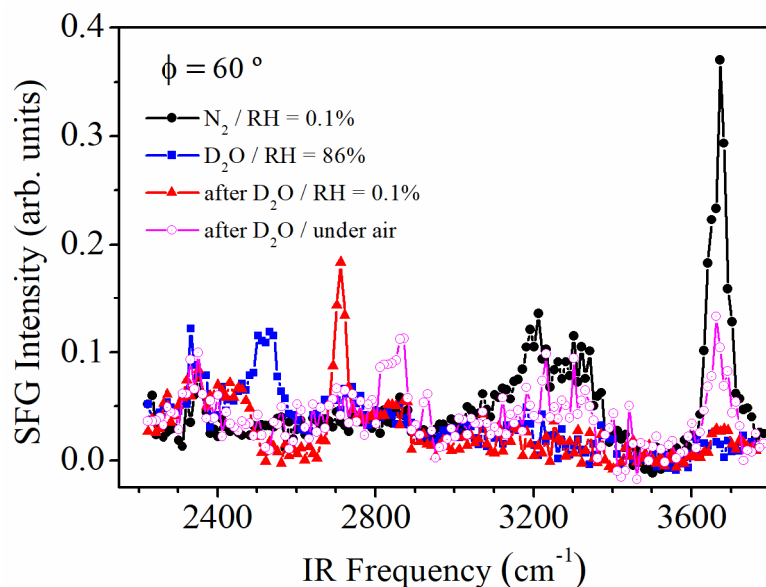


Fig. S5 – SFG spectra for the gypsum (010)/vapor interface in the OD and OH stretch ranges for a thick sample (only first surface reflection) with the azimuthal angle $\phi = 60^\circ$ and SSP polarization combination. Black dots are for the (010) surface under low humidity (RH = 0.1%), squares are measurements in equilibrium with D₂O vapor (RH = 86%), triangles are measured after D₂O adsorption and under dry conditions (RH = 0.1%), and empty circles are measured after D₂O adsorption and subsequent exposure to air (as in Fig. S4c).

5) Density profiles from AIMD simulations

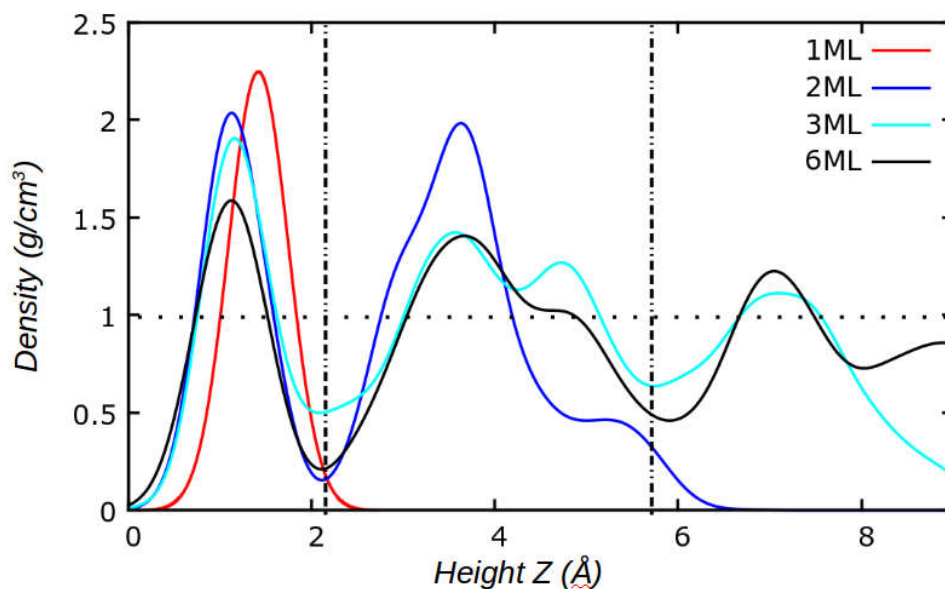


Fig. S6 – Water density as a function of the height Z for different coverages. The height of the outermost oxygen layer of gypsum was set as the zero reference ($Z = 0$). The dashed lines separate approximately each monolayer of adsorbed water. The dotted line is the experimental water density at room temperature.

6) Vibrational power spectra from AIMD simulations

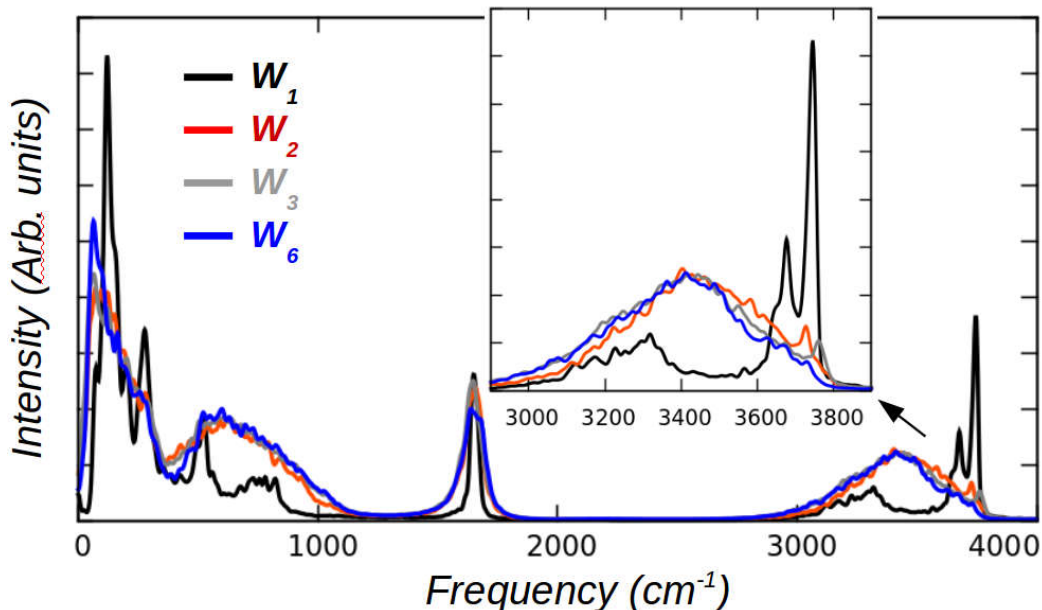


Fig. S7 – Surface water contribution to the power spectrum at 300 K for the 1ML, 2ML, 3ML and 6ML coverages. The intensities were normalized by the total number of water molecules.

7) Fitting of the SFG spectra for $\phi = 300^\circ$ and 330° for the gypsum (010) at RH = 0.1%.

The SFG spectra for $\phi = 300^\circ$ and 330° for the gypsum (010) surface under N_2 atmosphere was fitted to Eq. (1) for determining the relative signs of the mode amplitudes for the four different OH groups on the surface. The lower frequency modes corresponding to H-bonded OH groups (δ_2 , δ_4) were set to have the same sign, because otherwise the line shape in that frequency range would be obviously wrong. In Fig. S8 we show both experimental spectra fitted simultaneously to four resonances (with the same frequencies and line widths in all panels), but in each panel the relative signs of their amplitudes are different (as indicated in the figure). If we pay close attention to the qualitative agreement of the fitted *line shape* to the experimental one, we observe that the fitted curve displays the wrong line shape in the shaded regions of panels (a) and (c). In panel (a), the all-positive peaks display a destructive interference between δ_4 and δ_3 , leading to a deeper valley that is not observed experimentally. In panel (c), δ_1 and δ_3 with opposite signs make the valley between these peaks too shallow. The best fit with respect to the global line shape is obtained with the peaks due to (δ_2 , δ_4) with opposite sign with respect to (δ_1 , δ_3), and each pair with the same signs, shown in panel (b). Therefore, both free OH groups on average point away from the surface, while the H-bonded OH groups point down toward the $CaSO_4$ layer.

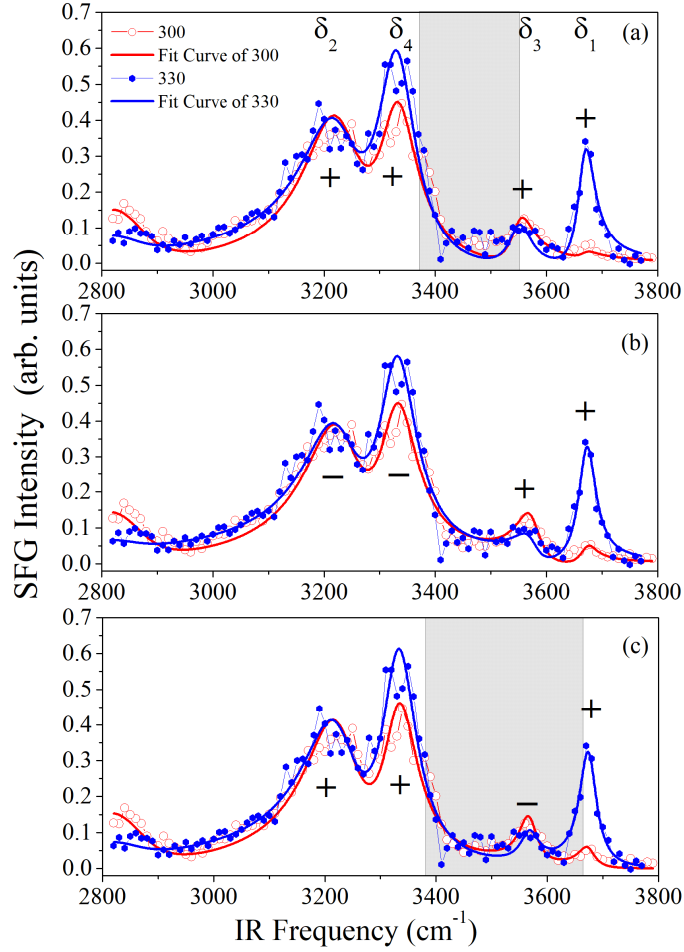


Fig. S8 – SFG spectra with SSP polarization combination for the gypsum (010) surface under N_2 atmosphere at azimuthal orientations $\phi = 300^\circ$ and $\phi = 330^\circ$. The spectra are fitted simultaneously to four resonances (with the same frequencies and line widths in all panels), but in each panel the relative signs of their amplitudes are different (as indicated in the figure).

8) Molecular orientation model for the SFG amplitude of OH groups

The $\chi^{(2)}$ tensor elements for a molecular interface is obtained from a coordinate transformation of the molecular hiperpolarizability $\alpha^{(2)}$ from the molecular frame (a, b, c) to the laboratory frame (X, Y, Z), where the incidence plane is (X, Z) and N is the surface density of molecules, as shown in equation S1.³

$$\chi_{ijk}^{(2)} = N \sum_{lmn} \langle (\hat{i} \cdot \hat{l})(\hat{j} \cdot \hat{m})(\hat{k} \cdot \hat{n}) \rangle \alpha_{lmn}^{(2)} \quad (\text{S1})$$

As the H-bonded (δ_2, δ_4) and free OH groups (δ_1, δ_3) of each surface water molecule at the dry gypsum (010) surface give separate contributions to the SFG spectra (uncoupled vibrations), we will consider each of them individually as an isolated group. Fig. S9 shows the OH group orientation (OH bond along the c axis, and the a axis in the XY plane) with respect to the lab frame, defining the polar angle θ of the OH bond with respect to the surface normal (Z) and its azimuthal angle ϕ with respect to the incidence plane (XZ).

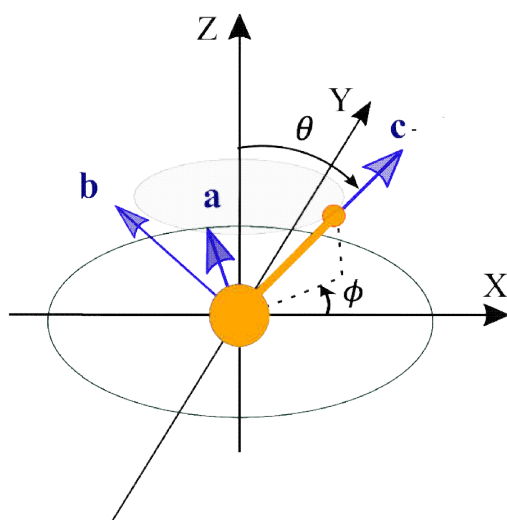


Fig. S9 – Definition of the OH group orientation (θ , ϕ) with respect to the laboratory frame (X, Y, Z). The molecular frame (a, b, c) is taken with c along the OH bond and a on the XY plane.

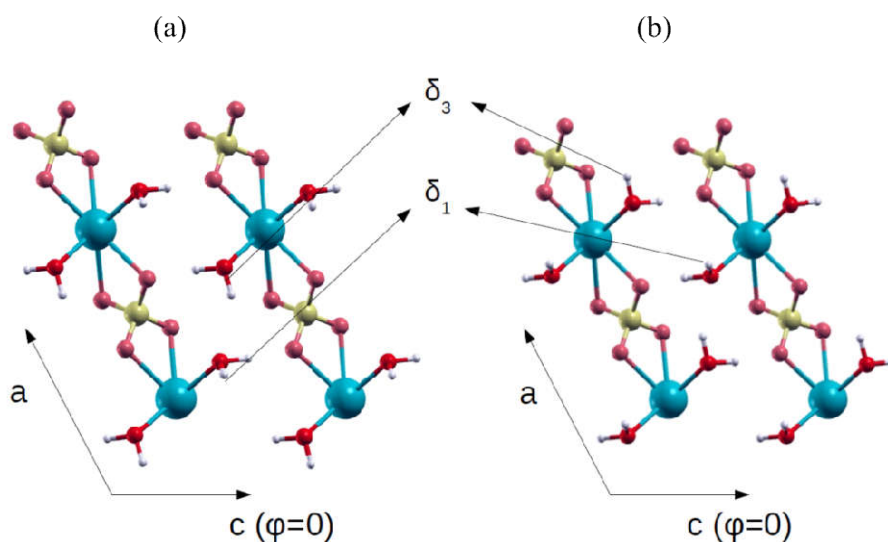


Fig. S10 – Two equivalent structures for the surface water molecules of the dry gypsum (010) surface.

The measured SFG spectra with SSP polarization combination probes two elements, $\chi_{yyz}^{(2)}$ and $\chi_{yyx}^{(2)}$. Considering OH groups with a specific orientation (θ , ϕ), the surface will have a C_{1v} symmetry and both of these $\chi^{(2)}$ elements would be nonvanishing. However, this would lead to a “forward-backward” asymmetry of the SFG amplitude as a function of azimuthal angle, $A(\phi) \neq A(\phi + 180^\circ)$, which is not observed in the data of Fig. 3b. Indeed, the AIMD simulations confirm that there are two surface configurations of water molecules that are energetically equivalent (~ 0.03 meV of total energy difference in a simulation cell), which correspond to exchanging the molecules that have the OH group pointing up (δ_1), and they have each type of OH group pointing in the opposite azimuthal direction, as displayed in Fig. S10. Hence, there is no macroscopic preference for azimuthal alignment of each type of OH group along ϕ with respect to $\phi + 180^\circ$, and the overall surface symmetry is increased to C_{2v} , for which $\chi_{yyx}^{(2)}$

vanishes. Therefore, the SSP spectra are probing only $\chi_{yyz}^{(2)}$, which will be expressed in terms of the molecular hyperpolarizability elements.

The molecular hyperpolarizability can be related to the product of the Raman tensor (β) and the IR transition dipole moment (μ) of the particular vibration (in our case, the OH stretch).

$$\alpha_{lmn}^{(2)} \propto \beta_{lm} \mu_n \quad (\text{S2})$$

Due to the C_∞ symmetry of the OH group, the hyperpolarizability nonvanishing elements are:

$$\alpha_{bbc} = \alpha_{aac} = r\alpha_{ccc}, \quad (\text{S3})$$

where r is the ratio of the Raman tensor elements perpendicular and along the bond direction. In principle it could be determined from Raman depolarization measurements, but a precise evaluation is difficult.⁴ Therefore, we will treat it as an unknown parameter that could be obtained from fitting the experimental SFG data (Fig. 3b).

From equation S1 and using the hyperpolarizability elements of equation S3, we get

$$\chi_{yyz}^{(2)} = \left\langle \cos \theta \left[r + (1 - r) \sin^2 \theta \sin^2 \phi \right] \right\rangle \alpha_{ccc}, \quad (\text{S4})$$

which may be written as

$$\chi_{yyz}^{(2)} = C \left[1 + D \sin^2 \phi \right], \text{ with } \begin{cases} C = r \cos \theta \alpha_{ccc} \\ D = \left(\frac{1-r}{r} \right) \sin^2 \theta \end{cases} \quad (\text{S5})$$

Equation S5 shows that (for $D > 0$, that is, $r < 1$) the SFG amplitude would be minimum when the OH group is along the incidence plane ($\phi = 0$), and maximum when its azimuthal orientation is perpendicular to the incidence plane ($\phi = 90^\circ$). Therefore, the direction of minimum amplitude in Fig. 3b gives directly the average azimuthal orientation ϕ_0 for that type of OH group (H-bonded or free OH), and fitting the shape of the azimuthal plot to Eq. S5 (with ϕ replaced by $\phi - \phi_0$) gives ϕ_0 and the parameter D , which depends both on r and the polar angle θ of that OH group. From the fits, $D = 3.6 \pm 1.6$ for the H-bonded OH (δ_2, δ_4) and $D = 4.2 \pm 1.5$ for the free OH (δ_1), while the ϕ_0 values are listed in Table 3 of the main paper. Using the average tilt $\theta_{2,4} \cong 106^\circ$ for (δ_2, δ_4) and $\theta_1 \cong 24^\circ$ for δ_1 from the AIMD simulation (Fig. 5a), we can obtain an estimate for r . The value $r = 0.20 (+0.11, -0.05)$ obtained for the H-bonded OH is close to those in the literature,⁵ while for the free OH we get a significantly smaller value, $r = 0.06 \pm 0.02$. This could result from the tighter OH bond for the free OH group, which could lead to a reduced transverse bond polarizability.

9) Polarization dependence of the SFG spectra for the gypsum (010) surface at low RH

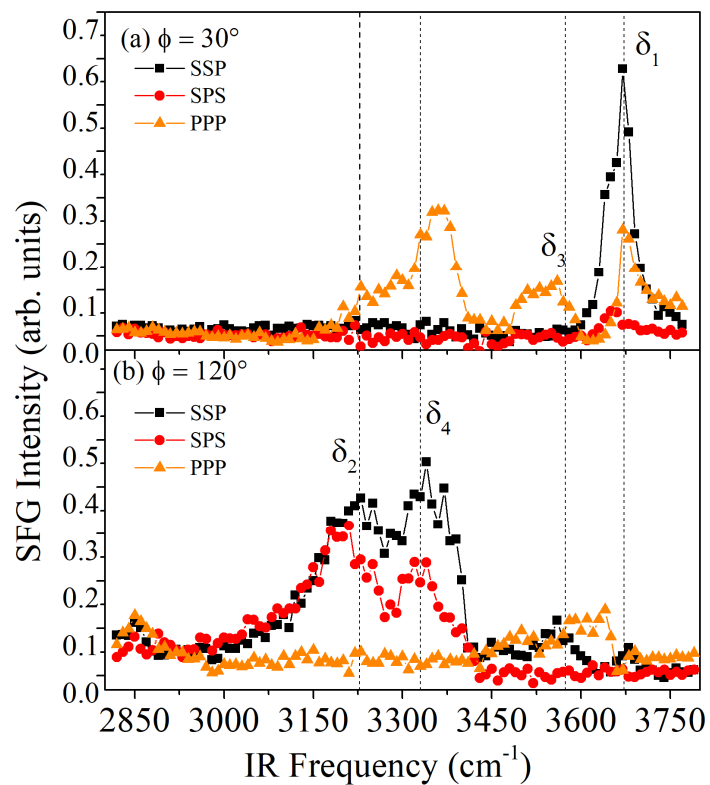
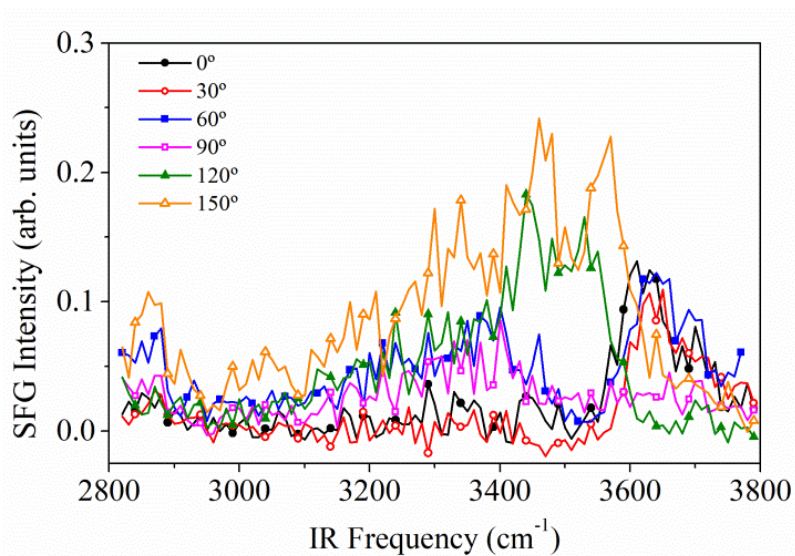
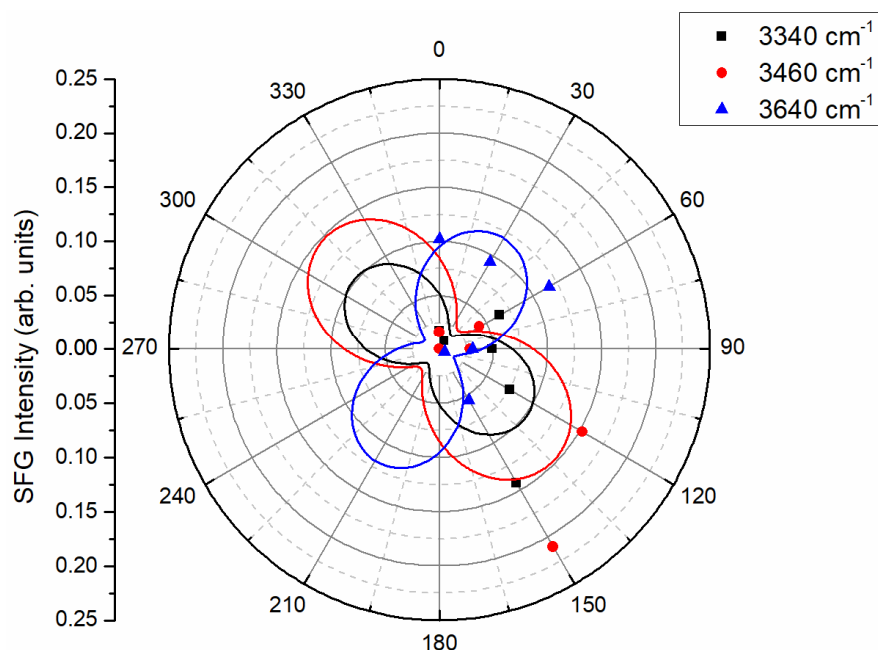


Fig. S11 – Polarization dependence of the SFG spectra for the gypsum (010) surface cleaved under N_2 atmosphere, RH 0.1%. The spectra were recorded at two azimuthal angles ϕ indicated in the panels.

10) Anisotropy of the adsorbed water on the gypsum (010) surface



(a)



(b)

Fig. S12 – (a) SFG spectra for the gypsum (010) surface under high relative humidity ($RH \approx 98\%$) at several azimuthal angles ϕ , with polarization combination SSP. (b) Azimuthal dependence of the SFG intensity for the spectra in (a), at the three frequencies indicated in the graph. The solid lines are fits using Eq. S5 (with ϕ replaced by $\phi - \phi_0$) and $I_{SSP} \propto |\chi_{yyx}^{(2)}|^2$. The fitting parameters ϕ_0 (the average azimuthal direction of the OH group) and D are listed in Table S1.

Table S1 - Fitting parameters for the azimuthal plots in Fig. S12(b).

Frequency (cm^{-1})	ϕ_0 ($^\circ$)	D
3340	39 ± 18	5.0 ± 12.2
3460	44 ± 16	5.0 ± 11.7
3640	119 ± 8	6.6 ± 8.6

REFERENCES

- (1) Shen, Y. R. Surface Contribution versus Bulk Contribution in Surface Nonlinear Optical Spectroscopy. *Appl. Phys. B* **1999**, *68* (3), 295–300.
- (2) Miranda, P. B.; Xu, L.; Shen, Y. R.; Salmeron, M. Icelike Water Monolayer Adsorbed on Mica at Room Temperature. *Phys. Rev. Lett.* **1998**, *81* (26), 5876–5879.
- (3) Zhuang, X.; Miranda, P. B.; Kim, D.; Shen, Y. R. Mapping Molecular Orientation and Conformation at Interfaces by Surface Nonlinear Optics. *Phys. Rev. B* **1999**, *59* (19), 12632–12640.
- (4) Wang, H.-F.; Gan, W.; Lu, R.; Rao, Y.; Wu, B.-H. Quantitative Spectral and Orientational Analysis in Surface Sum Frequency Generation Vibrational Spectroscopy (SFG-VS). *Int. Rev. Phys. Chem.* **2005**, *24* (2), 191–256.
- (5) Wei, X.; Miranda, P. B.; Zhang, C.; Shen, Y. R. Sum-Frequency Spectroscopic Studies of Ice Interfaces. *Phys. Rev. B* **2002**, *66* (8), 85401.